Development 140, 617-626 (2013) doi:10.1242/dev.085969

Kif5b controls the localization of myofibril components for their assembly and linkage to the myotendinous junctions

Zai Wang[1,2], Ju Cui[1,3], Wai Man Wong[4], Xiuling Li[1], Wenqian Xue[1], Raozhou Lin[1], Jing Wang[1], Peigang Wang[5], Julian A. Tanner[1], Kathryn S. E. Cheah[1], Wutian Wu[4,*] and Jian-Dong Huang[1,*]

SUMMARY

Controlled delivery of myofibril components to the appropriate sites of assembly is crucial for myofibrillogenesis. Here, we show that kinesin-1 heavy chain Kif5b plays important roles in anterograde transport of α-sarcomeric actin, non-muscle myosin IIB, together with intermediate filament proteins desmin and nestin to the growing tips of the elongating myotubes. Mice with *Kif5b* conditionally knocked out in myogenic cells showed aggregation of actin filaments and intermediate filament proteins in the differentiating skeletal muscle cells, which further affected myofibril assembly and their linkage to the myotendinous junctions. The expression of Kif5b in mutant myotubes rescued the localization of the affected proteins. Functional mapping of Kif5b revealed a 64-amino acid α-helix domain in the tail region, which directly interacted with desmin and might be responsible for the transportation of these proteins in a complex.

KEY WORDS: Kif5b, Desmin, Nestin, Myofibrils, Myotendinous junctions

INTRODUCTION

Although significant progress has been made in understanding the structure of skeletal muscle, the molecular mechanisms by which morphological rearrangements occur during myogenesis are less clear. Microtubules and actin filaments have been shown to be active in generating the spatial organization in differentiating muscle cells (Antin et al., 1981; Holtzer et al., 1975; Siebrands et al., 2004; Toyama et al., 1982). A panel of kinesin-related motor proteins has been suggested to be involved, including Kif1b/c (Dorner et al., 1998; Faire et al., 1998), Kif3a/b/c (Ginkel and Wordeman, 2000) and Kif5b (Rahkila et al., 1997). Among them, Kif5b, the ubiquitously expressed isoform of kinesin-1 heavy chain, is abundant in intestine, heart and skeletal muscle (Hollenbeck, 1989). A study based on physical training showed that variation in the *KIF5B* sequence could affect the ability of the heart to adjust to regular exercise in humans, indicating a potential role of kinesin-1 in cardiac muscle capability (Argyropoulos et al., 2009). One of the possible reasons for the kinesin-1-associated phenotype in muscle is thought to be related to the mitochondria, as Kif5b is responsible for anterograde mitochondrial movement by interacting with the mitochondrial protein Miro through the linker protein Milton (Wang and Schwarz, 2009). Another possible reason might be the Kif5b-dependent localization of nuclei, which is important for muscle activity. As demonstrated in a recent study, Kif5b directly interacts with Map7 to regulate the positioning of nuclei in differentiating myotubes (Metzger et al., 2012). Kinesin-1 has also been shown to interact with nesprin 4 through kinesin light chain (KLC) to regulate the localization of nuclei in several cell types (Roux et al., 2009), but whether this occurs in myogenesis needs further investigation. Immunostaining against kinesin heavy chain (KHC) showed that it might also function in ER-Golgi trafficking in skeletal muscles (Rahkila et al., 1997). However, the function of Kif5b in myofibrillogenesis and myotendinous junction (MTJ) formation has not been investigated.

During myofibrillogenesis, the myofibril components are transported to their appropriate sites for myofibril assembly. As suggested by Sanger et al., assembly begins at the edges of myotubes where Z-bodies, actin thin filaments and non-muscle myosin II (NMIIB) proteins form premyofibrils, which mature into myofibrils with the myosin isoform changed into muscle myosin II in the shaft of myotubes (reviewed by Sanger et al., 2005). However, the spatial control of the myofibrillogenesis has not been investigated. During myogenesis, the intermediate filament (IF) proteins desmin and nestin are also transported to the growing tips of the myotubes (Towler et al., 2004), where they represent the sites of the myotendinous junctions after maturation. In parallel to the MTJ complex, which includes integrins, talin and vinculin, IF proteins form physical links between the sarcomeric units and the sarcolemma (Carlsson et al., 1999; Tidball, 1992). Conventional kinesin has been suggested to play a role in transportation of vimentin in fibroblasts (Kreitzer et al., 1999; Prahlad et al., 1998), and neurofilament subunits in neural cells (Xia et al., 2003; Yabe et al., 1999). However, whether kinesin-1 is involved in the transportation of desmin and nestin during myogenesis has never been investigated.

To understand the role of Kif5b in muscle development and function, we generated mice with *Kif5b* conditionally knocked out in skeletal muscles. The mutant mice showed severe muscle dystrophy, exemplified by impaired myofibril assembly and their linkage to the myotendinous junctions, with myofibril components and IF proteins aggregated in the cell body. *In vitro*-differentiated myoblasts with Kif5b deficiency reproduced the *in vivo* phenotypes, and further demonstrated a role of Kif5b in anterograde transport of α-sarcomeric actin and NMIIB, together with the IF proteins desmin and nestin during myogenesis. Detailed mapping revealed that a 64-amino acid α-helix domain of Kif5b

[1]Department of Biochemistry, Li Ka Shing Faculty of Medicine, The University of Hong Kong, Hong Kong. [2]Institute of Clinical Medical Sciences, China-Japan Friendship Hospital, Beijing, China. [3]Beijing Institute of Geriatrics, Beijing Hospital, Ministry of Health, Beijing, China. [4]Department of Anatomy, Li Ka Shing Faculty of Medicine, The University of Hong Kong, Hong Kong. [5]HKU-Pasteur Research Centre, The University of Hong Kong, Hong Kong.

*Authors for correspondence (wtwu@hkucc.hku.hk; jdhuang@hkucc.hku.hk)

Accepted 20 November 2012

directly bound to desmin, and was responsible for the transportation of these proteins in a complex.

MATERIALS AND METHODS

Mouse strains

Kif5b$^{fl/}$ and *Kif5b*$^{+/-}$ mice have been described elsewhere (Cui et al., 2011). *Pax2-Cre* mice were provided by Dr A. K. Groves (Ohyama and Groves, 2004). *Kif5b*$^{+/-}$ mice were crossed with *Pax2-Cre* mice to generate *Kif5b*$^{+/-}$*:Pax2-Cre* mice. *Z/EG* (Novak et al., 2000) reporter mice were crossed with *Pax2-Cre* mice to generate the *Pax2-Cre:Z/EG* mice.

Antibodies and molecules for labeling

Kif5b antibody has been described elsewhere (Cui et al., 2011). Other antibodies and molecules for labeling were as follows: anti-myosin II (skeletal fast) (Sigma), anti-actin (Sigma), anti-KLC (a gift from Dr S. T. Brady, University of Illinois at Chicago, USA), anti-myoD (Santa Cruz), anti-α-sarcomeric actin (Covance), anti-GAPDH (Abcam), anti-α-tubulin (Sigma), anti-vimentin (Sigma), anti-dystrophin (Sigma), anti-NMIIB (a gift from Dr Adelstein, NIH, Bethesda, MD, USA; and from Covance), anti-desmin (Sigma), anti-talin 2 (Abcam), anti-integrin β1 (BD Transduction Labs), anti-His tag (Santa Cruz), anti-GM130 (BD Transduction Labs), anti-α-actinin (Sigma), anti-nestin (BD Transduction Labs), α-bungarotoxin conjugated with Alexa Fluor 488 (Molecular Probes) for AChR labeling, Phalloidin conjugated with rhodamine (Sigma) for F-actin labeling, Mitotracker (Molecular Probes) for mitochondria labeling and Lysotracker (Molecular Probes) for lysosome labeling. BrdU staining was performed using a Zymed BrdU staining kit according to the protocol.

DNA and RNA manipulation

Mouse *Kif5b* cDNA was kindly provided by Dr S. T. Brady. For Kif5b expression vectors in mammalian cells, Kif5b fragments were generated by PCR and cloned into pcDNA3.1 in *Bam*HI/*Not*I. For HA-tagged constructs, an HA tag was first cloned into pcDNA3 vector in *Xho*I/*Xba*I to generate pcDNA3-3′HA. Kif5b fragments were then cloned into pcDNA3-3′HA vector in *Bam*HI/*Not*I. For Kif5b without a KLC-binding domain (788-854 amino acids), Kif5b fragment (851-2363 nucleotides) was generated by PCR using the following primers: CAGAATTCTT-CAAGATTCATTA (forward; *Eco*RI) and GATAGATCTGTCTCCT-CCAAACCCTTC (reverse; *Bgl*II), and ligated into pcDNA3-Kif5b-HA (1-963 amino acids) cut with *Eco*RI/*Bgl*II to replace 851-2561 nucleotides. For GST-tagged Kif5b constructs, Kif5b fragments were cloned into pGEX-4T-1 vector in *Bam*HI/*Not*I (1-430 amino acids) or *Eco*RI/*Not*I. For desmin constructs, full-length desmin was generated by RT-PCR from myoblast cDNA. For EGFP-tagged desmin, the desmin gene was subcloned into pEGFP-C1 in *Bgl*II/*Eco*RI. For the His-tagged desmin construct, desmin was cloned into pET28a in *Bam*HI/*Eco*RI. RT-PCR primers for Pax2 are: 5′-CAGCCTTTCCACCCAACG; 3′-GTGGCG-GTCATAGGCAGC. Primers for GAPDH are: 5′-TCCCACTCTTCC-ACCTTCGATGC; 3′-GGGTCTGGGATGGAAATTGTGAGG.

Microscopy

For electron microscopy, 1 mm^3 cubes of tongue, forelimb, hindlimb and diaphragm muscles from newborn mice were fixed in 2.5% glutaraldehyde and 2% paraformaldehyde in 0.1 M sodium cacodylate (pH 7.4) at 4°C overnight, and then postfixed in 1% osmium tetroxide (OsO_4) in cacodylate buffer for 1 hour at room temperature. The samples were embedded in fresh epoxy resin. Semi-thin sections (1 μm) were cut, stained with Toluidine Blue and examined under a light microscope. Ultrathin sections were cut with Ultrcut S ultramicrotome (Reichert-Jung, Leica) and stained with uranium acetate and lead citrate. Sections were examined on a Philips EM208s transmission electron microscope operated at 80 kV. For fluorescence microscopy, images were captured using an Olympus BX51 fluorescence microscope or a Carl Zeiss LSM700 confocal microscope. A fluorescence recovery after photobleaching (FRAP) assay was performed using a Carl Zeiss LSM 510 Meta confocal microscope.

Primary culture of myoblast cells

The muscle from newborn hind limb was picked out in very small pieces by forceps and digested in 5 ml PBS plus 1 ml collagenase/dispase/$CaCl_2$ at 37°C for 20-30 minutes in shaking water bath. After preplatement in a tissue culture dish for 1 hour to remove the fibroblasts, the unattached cells were transferred to a 0.5% gelatin-coated dish in DMEM with 20% FBS and 2.5 ng/ml bFGF (Promega). Differentiation was promoted by changing medium to DMEM with 3% horse serum (Rando and Blau, 1994). For immunofluorescence staining, myoblast cells were seeded in eight-well chamber slides (Nunc) coated with 100 μg/ml poly-L-orthinine (Sigma), followed by 10 μg/ml laminin (Sigma) at 37°C overnight in a humidified incubator.

GST pull-down

For GST pull-down, the GST fusion proteins were expressed in BL21 *E. coli* cells overnight at 16°C after 0.5 mM IPTG induction. *E. coli* culture (5 ml) was collected and resuspended in 1 ml PBS buffer with protease inhibitors, and then sonicated for 3 minutes (5 seconds on/9 seconds off) to release the soluble fusion proteins. The *E. coli* cell debris were removed by centrifugation at 12,000 ***g*** for 30 minutes at 4°C, and the crude fusion protein solution were incubated with 40 μl glutathione-Sepharose 4B beads (Amersham Pharmacia Biotech) for 1 hour at 4°C. Myoblast cells (3×10^6) in a 10 cm dish differentiated for 2 days were washed with PBS and lysed by 1 ml ice-cold TNET lysis buffer [50 mM Tris-Cl (pH 7.4), 150 mM NaCl, 1 mM EDTA, 1% Triton X-100, 1 mM DTT and protease inhibitor cocktail (Roche)]. The lysate was then centrifuged at 12,000 ***g*** for 20 minutes at 4°C to remove the debris. GST proteins were incubated with the cell lysate for 4 hours at 4°C. For GST pull-down with desmin expressed from *E. coli*, desmin with a His tag was expressed in BL21 cells in the same way as GST-Kif5b fusion proteins. The cells were lysed in TNET lysis buffer, and the soluble fraction was incubated with GST-Kif5b fusion proteins pre-bound to glutathione-sepharose 4B beads.

Quantitative and statistical analysis

To quantify the percentage of cell tip distribution of fluorescence intensity, 30 cells were randomly selected in each group as indicated in the text. Photoshop was used to quantify the mean value of fluorescence intensity and the number of pixels in the selected regions. Student's *t*-test (two-sample unequal variance) was used to compare the statistical difference between the untransfected mutant group and other groups. $P<0.01$ was considered significant.

RESULTS

Generation of *Kif5b* conditional knockout mice by using *Pax2-Cre*

We have described a *Kif5b*^{fl} allele suitable for *Kif5b* gene inactivation using the Cre-loxP system (Cui et al., 2011). The strategy was to delete exon 2 of *Kif5b*, which contains an ATP/GTP-binding motif A (P-loop) crucial for ATP binding and kinesin motor activity, causing a frame-shift of the subsequent coding sequence.

To delete *Kif5b*, we first crossed heterozygous *Kif5b* (*Kif5b*$^{+/-}$) mice with mice carrying *Cre* gene downstream of a *Pax2* promoter (*Pax2-Cre*) (Ohyama and Groves, 2004) to generate a *Kif5b*$^{+/-}$*:Pax2-Cre* mice. Reported *Pax2-Cre* expression sites include kidney, mid-hindbrain, inner ear and spinal cord (Ohyama and Groves, 2004). However, when *Pax2-Cre* mice were crossed with *Z/EG* reporter mice (Novak et al., 2000), fluorescence was detected in tongue, pectoral muscles, limb muscles and diaphragm muscles (supplementary material Fig. S1A); but no fluorescence was detected in heart, lung, intercostal muscles or digestive system in newborn mice (data not shown). In order to further test whether Pax2-Cre was expressed in the skeletal muscle lineages, we carried out double labeling of EGFP and myosin II in the *Pax2-Cre:Z/EG* newborn mice. The EGFP signal was positive in the skeletal muscle cells labeled with myosin II, showing that the skeletal muscles were derivatives of Pax2-Cre expressing cells (supplementary material Fig. S1B).

We next generated *Kif5b*$^{fl/-}$*:Pax2-Cre* mice by crossing *Kif5b*$^{+/-}$*:Pax2-Cre* mice with *Kif5b*$^{fl/fl}$ mice (Cui et al., 2011). Although the wild-type and *Kif5b* heterozygous newborn mice quickly started to breathe and turned pink, some of the conditional knockout (termed as mutant) mice (*Kif5b*$^{fl/-}$*:Pax2-Cre*) could not develop normal breathing, characterized by noninflated lungs (supplementary material Fig. S1C). They died within minutes with blue bodies. Other mutant mice developed weak breathing and could live for about 1 day, but finally died with empty stomachs. One prominent phenotype consistently observed in all mutant mice was severe limb muscle dystrophy, which could be used to distinguish mutant mice from their littermates by naked eyes (Fig. 1A). The reduced skeletal muscle amount was also demonstrated in hindlimb sections (supplementary material Fig. S1D). In the mutant mice that could live for 1 day, no limb movement was observed even when struck with forceps, showing the dysfunction of these muscles.

Kif5b expression levels were examined in kidney, hindlimb and diaphragm muscles from newborn live mice by western blot (Fig. 1B), as well as by immunofluorescence on hindlimb muscles (Fig. 1C). Compared with the *Kif5b* heterozygous mice, the knockout efficiency was more than 80% in skeletal muscles in mutant mice. To confirm the tissue specificity of the *Kif5b* knockout, tissues from 16.5 dpc embryos were examined. *Kif5b* deficiency was also observed in kidney, tongue muscle and mid-hindbrain, but not in heart, cerebrum and lung, as expected (supplementary material Fig. S1E).

Kif5b mutant mice show severe skeletal muscle dystrophy

The skeletal muscle defects suggest that the neonatal death of mutant mice could be caused by the failure of diaphragm and pectoral muscles for breathing, as well as tongue and chewing muscles for milk intake. We thus focused on the roles that Kif5b may play in skeletal muscle development and function.

The mutant muscle fiber exhibited four major defects in structure analysis when compared with wild-type mice. The first defect is nuclei aggregation. During maturation of muscle development, nuclei move to the periphery of cells from the center of the myotubes (Gilbert, 2000). In wild-type limb muscle fibers, nuclei distributed evenly throughout the cell length, with most of the nuclei already having moved to the periphery. However, in mutant muscle fibers, the nuclei were centrally located (Fig. 1D,F).

The second defect is mitochondrial accumulation around nuclei, as shown in the diaphragm muscles of mutant mice (Fig. 1E). These observations are consistent with previous reports that Kif5b is responsible for nuclei and mitochondria localization (Metzger et al., 2012; Tanaka et al., 1998).

The third abnormality is in myofibril assembly in mutant mice, as revealed in ultrathin sections. In mutant diaphragm muscles, the myofibers assembled with light Z-discs and the M-lines were almost missing. In addition, the length of sarcomeric unit was shortened compared with that in wild-type muscles (Fig. 1E). In forelimb muscles, rudimentally assembled myofibrils or disassembled myofibril fragments were extensively presented. Only a few well-assembled myofibrils were observed. However, some of the H bands were not clear, and individual myofibrils were rudimentally aligned and loosely bundled (Fig. 1F).

The fourth abnormality is the shrunk ends of Kif5b-deficient muscle fiber, implying an unstable MTJ. Electron microscopy revealed that the integrin complex as shown in dense material on the sarcolemma was intact in mutant mice. However, the myofibril filaments cannot reach the end of muscle fiber; they appeared disorganized in the terminal region, and the lateral detachment of myofibrils with sarcolemma was also detected (Fig. 1G).

Taken together, these data showed that Kif5b deficiency in skeletal muscles caused severe morphological abnormalities, including nuclei and mitochondrial aggregation, impaired myofibril structure and MTJ. These defects may result in physical disability, indicating that Kif5b may have a role in generating or stabilizing the muscle cell organization.

Kif5b deficiency leads to aggregation of myofibril components and IF proteins

As the myofibril filament assembly was compromised in Kif5b-deficient muscles, we further examined the localization of myofibril components by immunofluorescence. Myosin II and actin formed repeated sarcomeric units in wild-type sections, whereas these two molecules aggregated inside the mutant cell body; myofibrils assembled only near the cell membrane (Fig. 1H), indicating that Kif5b was important for the proper localization and assembly of myofibril components. For muscle contraction, the integrity of both myofibril structure and neuromuscular junction (NMJ) is indispensable. In both wild-type and mutant muscle fibers, the acetylcholine receptor (AChR) that responds to the neurotransmitter acetylcholine and activates muscle contraction showed normal localization on sarcolemma (supplementary material Fig. S1F).

As IF proteins are important for forming physical links at the MTJ, we tested whether the localization of IF proteins at the area near the MTJ was affected by Kif5b deficiency. We first examined the presence of Kif5b in wild-type muscle fibers. Kif5b was localized around Z-discs throughout the cells and colocalized with desmin (Fig. 2A). At the area near the MTJ, Kif5b was distributed in a digit-like pattern and localized in the same region as desmin (Fig. 2B). Desmin expression was detected around Z-discs throughout the muscle fiber but was concentrated at MTJ, exhibiting digit-like patterns in wild-type muscles. However, desmin aggregated in the cell body near the nuclei in mutants (Fig. 2C, left panel). Similarly, nestin was stained weakly around Z-discs and strongly concentrated at the MTJ area in wild-type mice muscles and also displayed a digit-like pattern. However, nestin mislocalized in the mutant cell body with filamentous deposition (Fig. 2C, right panel). These data demonstrated that the localization of the IF proteins desmin and nestin was severely affected by Kif5b deficiency.

Kif5b knockout cells resemble *in vivo* abnormalities

Because Pax2-Cre was expressed in several other tissues besides skeletal muscle, we could not exclude the influence of potential defects in other tissues on the muscle phenotypes observed. To investigate the function of Kif5b in an isolated myogenesis process, we used primary cultured myoblast cells as an *in vitro* myogenesis model system. We extracted myoblast cells from wild-type (*Kif5b*$^{fl/+}$), heterozygous (*Kif5b*$^{fl/-}$) and mutant (*Kif5b*$^{fl/-}$*:Pax2-Cre*) mice. The identity of cultured myoblast cells was verified by the expression of MyoD at the proliferating stage (Fig. 3A). Kif5b was knocked out efficiently in myoblasts from mutant mice, as Kif5b was undetectable in these cells, whereas it was upregulated upon differentiation in wild-type cells (Fig. 3A). As a further line of evidence, KLC also diminished with Kif5b knock down in mutant cells (Fig. 3A). In addition, endogenous Pax2 was expressed in myoblast cells, but was

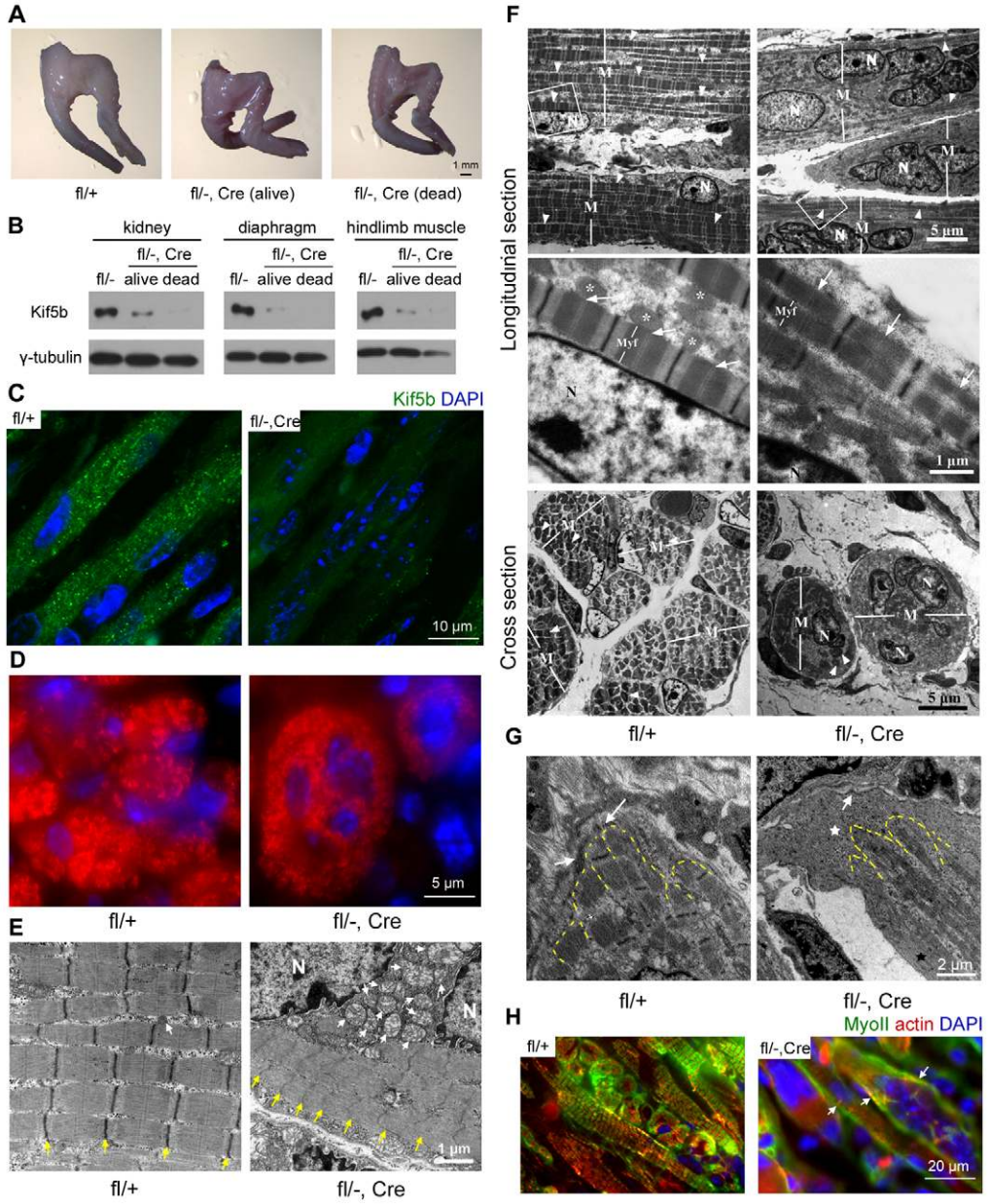

Fig. 1. *Kif5b* conditional knockout mice show severe skeletal muscle dystrophy. (**A**) Hindlimbs from newborn live and dead mutants (*Kif5b*$^{fl/-}$*:Pax2-Cre*) showed severe dystrophy compared with wild-type (*Kif5b*$^{fl/+}$) littermates. (**B**,**C**) Kif5b expression levels in newborn mutant mice were examined by western blot (B) or by immunofluorescence on hindlimb sections (C) in wild-type and mutant mice, as indicated. (**D**) Myosin II (red) and DAPI (blue) staining on hindlimb muscles of newborn mice in cross-sections. Centrally aggregated nuclei are prominent in mutant muscles. (**E**) Electron photomicrographs of diaphragm muscles from newborn mice in longitudinal section. In mutant muscle cell, two nuclei (N) were located close together, with large numbers of mitochondria (white arrows) aggregated between the nuclei. The myofibrils were poorly assembled, with only light Z-lines visible (yellow arrows). (**F**) Electron photomicrographs of skeletal muscles from forelimbs of newborn mice. Upper panels show longitudinal sections. M, muscle cells; N, nuclei. In mutant mice, only a few myofibrils were observed (arrowheads). Nuclei were located centrally in the cells. Middle panels are enlargements of the areas outlined in upper panels, showing the structure of myofibrils (Myf). Some of the H bands were not clear in mutant mouse (middle right, arrows) compared with that in wild-type mice (middle left, arrows). In addition, many mitochondria (asterisks) were found along the myofibrils in wild-type mice but not in mutant mice. Lower panels are cross-sections showing the muscle fibers (M), nuclei (N) and myofibrils (arrowheads). (**G**) Electron photomicrographs of the myotendinous junction (MTJ) region. In mutant muscles, the integrin complex in dense material on the sarcolemma was intact (white arrows). The ends of myofibrils (dashed yellow lines) could not reach the sarcolemma at the MTJ, leaving the adjacent area absent of myofibrils (white star). Lateral detachment of myofibrils with sarcolemma was also present (black star). (**H**) Tongue muscle sections were stained using anti-myosin II (green), anti-actin (red) and DAPI (blue). Myosin II and actin were assembled into repeated units in control cells, but distributed mostly in a diffused pattern in mutant cells.

undetectable in mature skeletal muscle tissues (supplementary material Fig. S2A), indicating that Cre activity was consistent with endogenous Pax2 expression.

Kif5b-deficient cells showed a faster growth rate than wild-type cells (supplementary material Fig. S2B), and had a normal cell cycle distribution, as demonstrated by FACS analysis

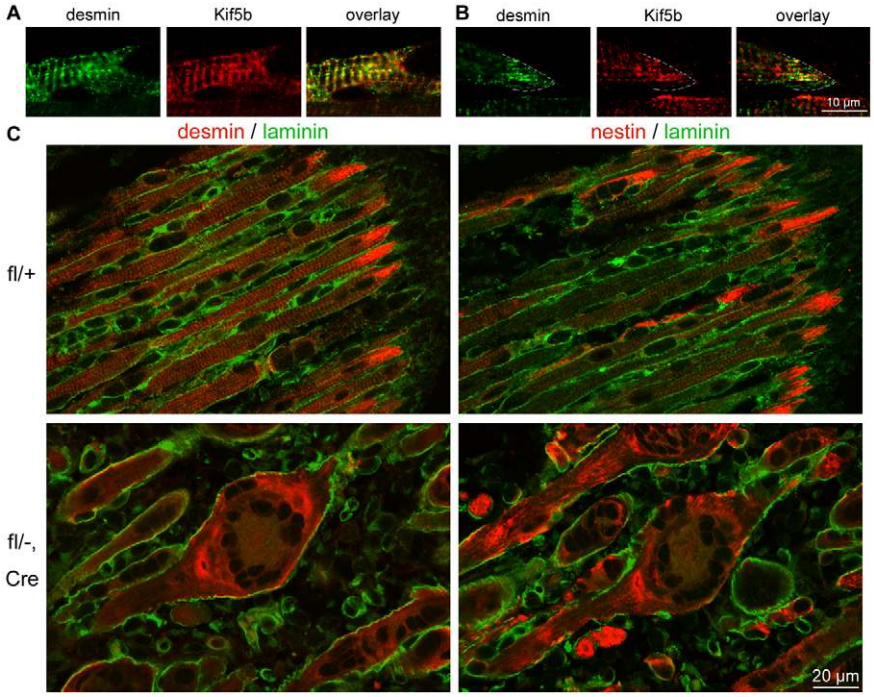

Fig. 2. Intermediate filaments mislocalize in Kif5b-deficient muscles. (**A**,**B**) Desmin and Kif5b colocalized around Z-discs (A) in hindlimb muscles from wild-type newborn mice and showed a digit-like pattern in the same area near the myotendinous junction (MTJ) (B). (**C**) Desmin or nestin double stained with laminin on hindlimb muscles. Desmin and nestin concentrate at the MTJ in wild-type muscles, but mislocalize in the cell body in mutant muscles.

(supplementary material Fig. S2C). They could exit the cell cycle and prepare for differentiation in response to growth factor depletion, as monitored by BrdU incorporation (supplementary material Fig. S2D), and expressed several differentiation markers normally on the third day after differentiation, including myosin II, α-sarcomeric actin and desmin (Fig. 3A). These data showed that the regulation of cell cycle and muscle-specific gene expression upon differentiation was not severely affected by *Kif5b* knockout.

To address the issue of whether cultured myoblast cells can reproduce the *in vivo* phenotypes, we first examined morphological changes during *in vitro* differentiation. The wild-type myoblasts fused into bipolar-shaped multi-nucleated myotubes on the third day after differentiation. The cells had a constant shaft diameter throughout the cell body, and the nuclei were distributed along the longitudinal axis. For the mutant myoblasts, the majority of cells maintained a bipolar shape but appeared shorter than wild-type cells, with multiple nuclei aggregating in the center of the enlarged cell body. The shaft shrunk rapidly from the center, leaving very thin cell shaft and tips at two ends (Fig. 3B).

Next, we examined myofibrils formation in differentiated myoblast cells. F-actin lay in parallel throughout the shaft in most wild-type cells. In some cells, F-actin formed small dots along a single fiber, representing the initiation of I-band formation. In other cells, a striated I-band pattern was visible. In mutant cells, besides normally formed parallel linear F-actins and striated fibers, there were many distorted F-actins wrapped around the centrally located nuclei, and aggregation was also visible (Fig. 3C). A-band formation was also tested using myosin II staining. In about 1% of the wild-type and mutant cells, the striated pattern can be observed. Abnormally aligned F-actin may affect A-band formation,

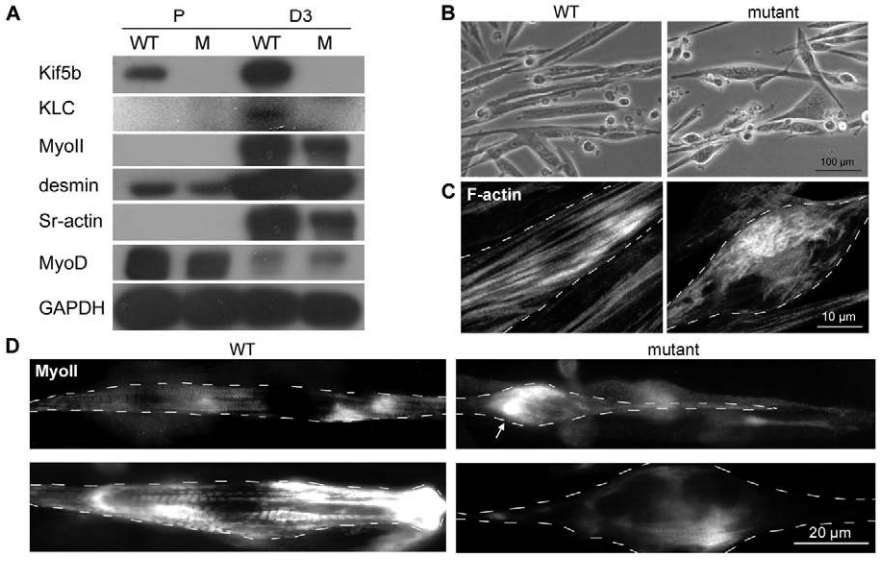

Fig. 3. *In vitro* differentiated myoblast cells reproduce *in vivo* abnormalities. (**A**) Proliferating myoblasts (P) and cells differentiated for 3 days (D3) were collected and subjected to western blot. GAPDH served as the loading control. WT, *Kif5b*$^{fl/+}$; M, *Kif5b*$^{fl/-}$*:Pax2-Cre*. (**B**) Light microscopy of wild-type and mutant myoblast cells differentiated for 3 days. (**C**,**D**) F-actin (C) or myosin II (D) were labeled in wild-type (left panel) or mutant (right panel) cells differentiated for 3 days. F-actin forms aggregates in mutant cells. For myosin II, two typical staining images are shown for both wild type and mutant. Aggregation in mutant cells is indicated by an arrow. Broken line shows one cell boundary.

indicated by myosin II aggregation in mutant cells (Fig. 3D). In some other mutant cells, only rudimentally assembled myosin II bands were detected (Fig. 3D).

Besides, we found severe mislocalization of Golgi and mitochondria in mutant cells. Some Golgi apparatus localized at the bipolar sites near the nuclear membranes in wild-type cells, and some others dispersed into the myotube shafts. However, Golgi formed ring-like pattern around the nuclear membranes in mutant cells and some moved into the invaginations of the nuclei. Little dispersion of Golgi into the mutant myotube shafts was observed (Fig. 4, left panel). By contrast, lysosomes showed similar distribution pattern in wild-type and mutant cells (Fig. 4, left panel). The mitochondria presented an anterograde dispersion pattern in wild-type cells; however, they accumulated around the centrally aggregated nuclei in mutant cells (Fig. 4, right panel). These data show that Kif5b plays significant role in the dispersion of nuclei, Golgi and mitochondria, as well as in myofibrillogenesis by affecting actin assembly. The abnormalities observed in mutant cells were consistent with *in vivo* results, demonstrating that these cells could recapitulate the Kif5b deficiency phenotypes and acted as a good model for studying the role of Kif5b in myogenesis.

Kif5b is responsible for the localization of α-sarcomeric actin, NMIIB, desmin and nestin in differentiating myoblast cells

Upon myoblast fusion, microtubules reorganize and become polarized in fused myotubes. The minus ends are embedded in the perinuclear materials and the plus ends direct towards the growing tips (Musa et al., 2003; Tassin et al., 1985). Kinesin-1, the plus-end-directed microtubule motor protein, was possibly involved in protein or vesicle transport towards the growing tips of the myotube. Besides organelles like nuclei, Golgi and mitochondria as mentioned above, we examined the localization of a panel of proteins in wild-type and mutant cells. The localization of several candidates, including muscle α-actinin in Z-discs, dystrophin and talin 2 in the submembrane area, and integrin β1 at cell-matrix interaction sites, was not severely affected (supplementary material Fig. S3A).

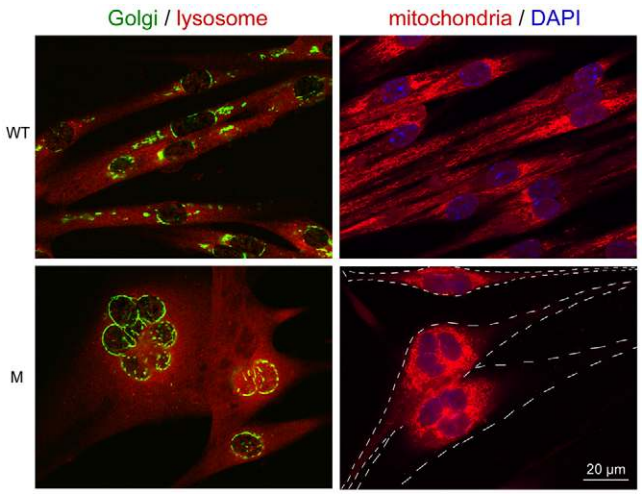

Fig. 4. Golgi and mitochondria mislocalize in Kif5b-deficient myoblast cells. Double labeling of Golgi and lysosome (left panels) or mitochondria labeling (right panels) were performed in myoblasts differentiated for 3 days. Golgi and mitochondria dispersion were disrupted in mutant cells. Broken lines show the boundaries of three mutant cells.

On the contrary, the localization of α-sarcomeric actin, NMIIB, desmin and nestin was affected by Kif5b deficiency. α-Sarcomeric actin and NMIIB are two key components in the formation of premyofibrils at the growing tips of the myotubes (reviewed by Sanger et al., 2005). α-Sarcomeric actin and NMIIB dispersed throughout the wild-type cells, with slight concentration at the tips in some of the cells. However, these two molecules tended to concentrate around the nuclei in mutant cells (Fig. 5A). The IF proteins desmin and nestin were expressed in the region near the nuclei, and then re-located specifically to the growing tips of the myotubes in wild-type cells (Towler et al., 2004). However, desmin and nestin severely aggregated around the nuclei in the mutant cells (Fig. 5A). To confirm that Kif5b was responsible for the localization of the affected proteins, we performed a rescue experiment by overexpressing Kif5b in the mutant cells. The expression of Kif5b promoted the dispersion of α-sarcomeric actin, NMIIB, desmin and nestin into the cell tip regions (Fig. 5B), confirming the role of Kif5b in the localization of these proteins in elongating myotubes. Unlike desmin or nestin, a third IF protein vimentin did not show cell tip-enriched localization in wild-type cells. Vimentin dispersed throughout the cells in both wild-type and mutant cells, and overexpression of Kif5b did not promote the transportation of vimentin to the mutant cell tips (supplementary material Fig. S3B).

To further demonstrate that desmin transport is dependent on Kif5b, we constructed EGFP-tagged desmin expression vector and transfected it into wild-type or mutant cells. Desmin-EGFP

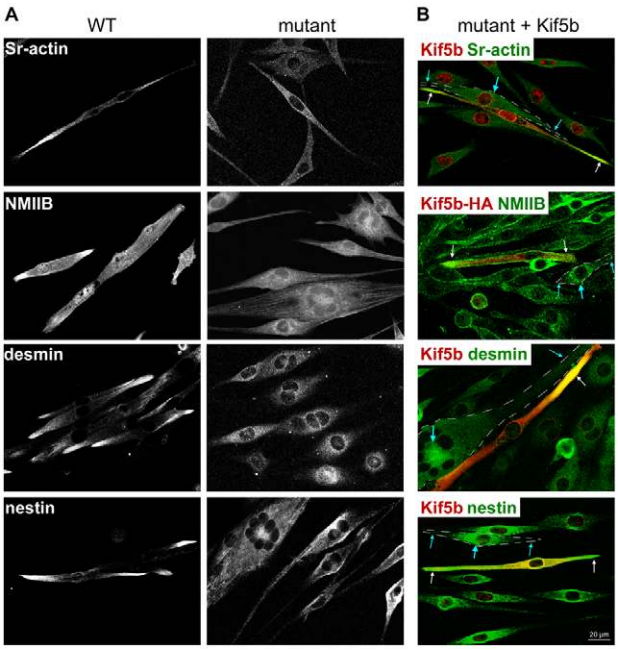

Fig. 5. Kif5b is responsible for the localization of α-sarcomeric actin, NMIIB, desmin and nestin. (**A**) Immunostaining of α-sarcomeric actin, NMIIB, desmin and nestin in wild-type (left panels) and mutant (right panels) cells differentiated for 2 days. The transportation of these proteins into the cell tips was affected by Kif5b deficiency. (**B**) Mutant cells were transfected with Kif5b or Kif5b-HA expression vectors upon differentiation, and then double labeled with anti-Kif5b or anti-HA together with anti-α-sarcomeric actin, -NMIIB, -desmin or -nestin, as indicated. Kif5b antibody showed slight background staining of the nuclei in mutant cells. Proteins concentrated around the nuclei (big blue arrows) in untransfected cells with cell tip localization missing or severely compromised (small blue arrows). In Kif5b transfected cells, cell tip localization of these proteins was restored (white arrows). Broken lines show the cell boundaries.

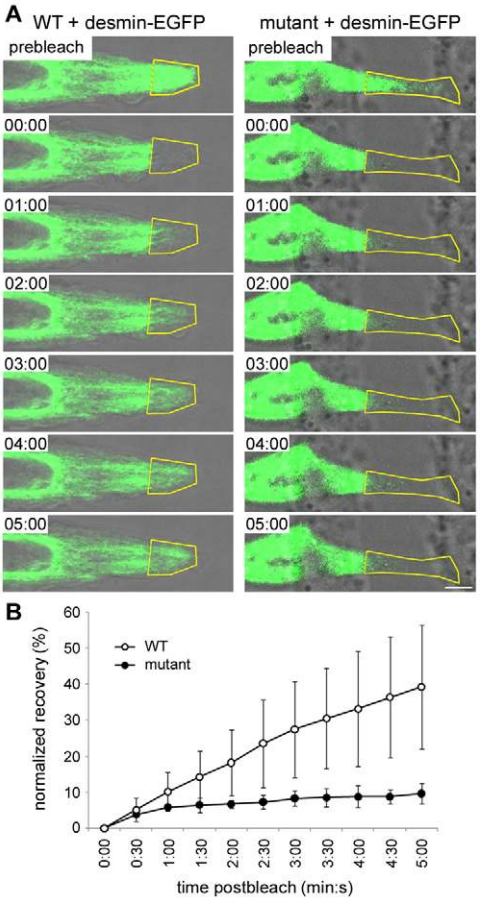

Fig. 6. FRAP assay of desmin-EGFP in wild-type and mutant cells. (**A**) Wild-type (left panels) and mutant (right panels) myoblast cells were transfected with desmin-EGFP and then differentiated for 2 days. The selected tip regions (yellow outlines) were photobleached. Images were captured at 30-second intervals for 5 minutes after photobleaching. Scale bar: 5 μm. (**B**) Normalized fluorescence recovery in the photobleached regions in wild-type (open circles) and mutant (filled circles) cells. The results were from three typical cells in each group and are normalized to the fluorescence intensity from the whole cell region. Data are mean±s.e.m.

dispersed into the wild-type myotube shafts and gradually accumulated at the cell tips. When we photobleached the tip region, the wild-type cells could recover about 40% of the fluorescence intensity in 5 minutes (Fig. 6A,B; supplementary material Movie 1). The small dots of fluorescence that may represent monomers or oligomers of desmin-EGFP exhibited fast transportation, moving at up to 50 μm/minute in wild-type cells. The transportation speed of filamentous desmin-EGFP was 6-18 μm/minute, belonging to a slow-to-medium transportation speed. The speed of desmin-EGFP transportation was comparable with other IF proteins in other cell types (Kreitzer et al., 1999; Prahlad et al., 1998; Xia et al., 2003; Yabe et al., 1999). The mutant cells showed severe defect in desmin-EGFP transportation. Most of the proteins localized around the cell nuclei; very weak fluorescence was visible in the tip region. When the tip region was photobleached, these mutant cells recovered only 10% of the original fluorescence intensity in 5 minutes (Fig. 6A,B; supplementary material Movie 2). As the desmin expression site is proximal to the nuclei (Towler et al., 2004), the replacement of desmin in the distal tip region is largely dependent on intracellular transport, indicating a role for Kif5b in desmin turnover in the cell tip region. Therefore, these data clearly show that desmin transportation to the cell tips is dependent on Kif5b.

Kif5b tail directly interacts with desmin

The C-terminal tail domain of Kif5b is proposed to interact with cargo proteins directly or through KLC (Diefenbach et al., 1998; Hirokawa et al., 1989; Kanai et al., 2004). To determine which region of the Kif5b tail domain controls the localization of the affected proteins, we constructed a series of Kif5b truncations with or without HA tag at the 3′ terminus and subjected them to functional analysis. Surprisingly, the functional domain in Kif5b for these four proteins (α-sarcomeric actin, NMIIB, desmin and nestin) was identical. Kif5b 1-890 amino acids was sufficient for localization of these proteins, however Kif5b 1-850 amino acids could not rescue their localization. However, Kif5b lacking the KLC binding domain (788-854 amino acids) was functional, confirming that the KLC-binding domain of Kif5b was dispensable for its function (Fig. 7A). Based on the construct without KLC-binding domain (dLCB-HA), we further mapped the minimal functional domain in the C-terminal tail region. The global domain in the tail contains mainly random coils (919-963 amino acids) and has been proposed to be a cargo protein-binding domain (Hirokawa et al., 1989; Yang et al., 1989). The 918-929 amino acid region contains the auto-inhibitory peptide (Dietrich et al., 2008; Kaan et al., 2011). Kif5b with the globular tail domain deletion (dLCB918-HA) was still functional. Further truncation of the 855-918 amino acid α-helix domain (dLCB904-HA) abolished Kif5b-mediated transportation of desmin, nestin and α-sarcomeric actin and NMIIB (Fig. 7A,B; supplementary material Fig. S4). As a control, we tried different Kif5b constructs on mitochondrial rescue experiments. Other than 855-918 amino acids, the KLC-binding domain (788-854 amino acids) was found to be important for mitochondrial transportation (supplementary material Fig. S4). The result was consistent with previous work suggesting that *D. melanogaster* KHC 811-891 amino acids is important for mitochondrial transportation (Glater et al., 2006). We calculated the percentage of tip distribution (Fig. 7C) of α-sarcomeric actin, desmin and nestin in 963-HA- (full-length Kif5b), dLCB-HA-, dLCB918-HA- and dLCB904-HA-transfected mutant cells, untransfected mutant cells and wild-type cells. As the NMIIB antibody showed a relatively higher background in nuclei, we did not quantify this protein. We found significant differences between Kif5b-963HA-, Kif5b-dLCBHA-, Kif5b-dLCB918HA-transfected mutant cells and untransfected mutant cells, but not between Kif5b-dLCB904HA-transfected mutant cells and untransfected mutant cells for the tip distribution of α-sarcomeric actin, desmin and nestin (Fig. 7D). Taken together, our data indicate that the 64 amino acids (855-918 amino acids) are responsible for the role of Kif5b in transporting α-sarcomeric actin, desmin and nestin.

We then tested whether the Kif5b tail domain has the capacity to bind to these cargo proteins by GST pull-down experiment. We first roughly dissected the full length of Kif5b into four fragments and incubated these GST fusion proteins with lysate from wild-type myoblasts differentiated for 2 days. GST-Kif850-963 could bind to desmin, α-sarcomeric actin and NMIIB, whereas GST-Kif679-890 bound to α-sarcomeric actin and NMIIB but not desmin. Muscle myosin II, as a negative control, cannot bind to GST-Kif5b fusion proteins (Fig. 8A).

As the tail of Kif5b or, more specifically, the 64-amino acid α-helix domain, is supposed to be functional, we asked whether this

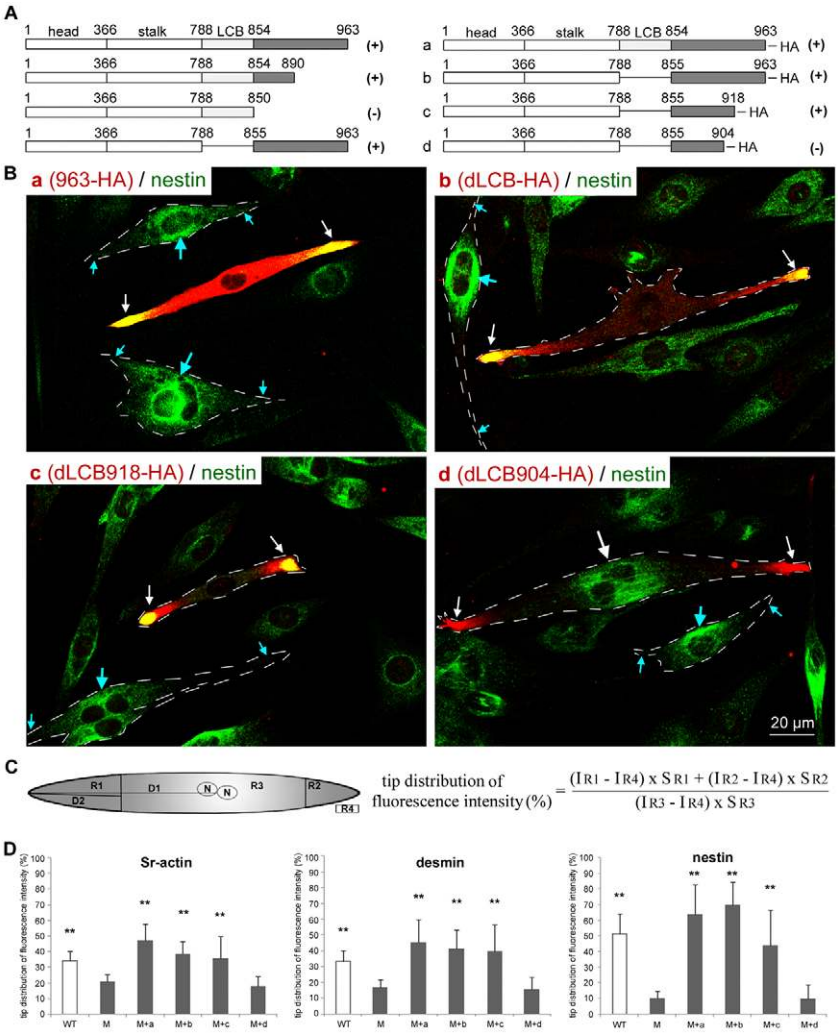

Fig. 7. Mapping of functional domain of Kif5b in protein transportation. (**A**) Kif5b constructs without or with HA tags were transfected into mutant cells upon differentiation to perform the rescue assays. + and – indicate the ability or inability, respectively, to restore the localization of affected proteins in mutant cells. LCB, light chain-binding domain. (**B**) Typical results of nestin rescue experiments using the constructs 963-HA (a), dLCB-HA (b), dLCB918-HA (c) and dLCB904-HA (d). 963-HA, dLCB-HA and dLCB918-HA could restore the tip localization of nestin, whereas construct dLCB904-HA could not. Big and small blue arrows indicate the areas near the nuclei and the tip regions, respectively, in untransfected cells. Big and small white arrows indicate the areas near the nuclei and the tip regions, respectively, in transfected cells. Dashed lines indicate cell boundaries. (**C**) Quantitative method used to determine the percentage of cell tip distribution of fluorescence intensity of the affected proteins. N, nuclei; D, distance; R, region (R1, tip region 1; R2, tip region 2; R3, total cell body region; R4, background region); I, mean value of fluorescence intensity in the selected region; S, number of pixels in the selected region. The tip regions were generally defined as D2=1/2 D1. (**D**) Quantitative analysis of the percentage of cell tip distribution of fluorescence intensity for α-sarcomeric actin, desmin and nestin in wild type (WT), in mutant (M) and in mutant cells transfected with Kif5b constructs (M+a, M+b, M+c, M+d), as indicated. **Significant difference between the target group and untransfected mutant group (P<0.01). Data are mean±s.e.m.

domain had the capacity of binding to the cargo proteins. As a result, the 64-amino acid domain (855-918 amino acids) had a similar binding capacity to the full-length tail (850-963 amino acids). As controls, a peptide composed of 850-890 amino acids or the global tail domain of 919-963 amino acids could not bind to the potential cargo proteins (Fig. 8B). These data indicated that Kif5b may form a complex with its cargo proteins through this 64-amino acid domain.

We also tried using mutant myoblast cell lysate in the GST pull-down assays. In this circumstance, only desmin can bind to GST-Kif855-918, but not α-sarcomeric actin or NMIIB (Fig. 8C). This result suggests that there should be other linker proteins, which were missing or abnormally functioning in mutant cells, bridged Kif5b tail and actin/NMIIB. We next tried to test whether Kif5b and desmin have a direct interaction. Data showed that 679-890 amino acids and 855-918 amino acids of Kif5b could bind to His-tagged desmin, whereas 919-963 amino acids could not (Fig. 8D). These data are consistent with the rescue experiments, indicating that Kif5b directly interacts with desmin through the α-helix domain in the tail, which is crucial for the Kif5b-mediated transportation of desmin, nestin, α-sarcomeric actin and NMIIB.

DISCUSSION

In this study, severe skeletal muscle dystrophy was observed in *Kif5b* conditional knockout mice. In particular, Kif5b plays significant roles in myofibrillogenesis and in MTJ stability. The myofibrils assembly was severely affected by Kif5b deficiency, with actin and myosin II aggregation observed in mutant muscles. For the MTJ stability, Kif5b deficiency led to the detachment of the myofibrils from the sarcolemma. The myofibrils could not reach the end of muscle fiber and appeared disorganized in the terminal region. The IF proteins desmin and nestin, which normally form physical links between the myofibrils and the MTJ, mislocalized in the mutant cell body. The defect in myofibril assembly and the inefficient linking of myofibrils to the MTJ area, in parallel with the aggregated nuclei and mitochondria, may together contribute to muscle dysfunction in Kif5b-deficient mice muscles.

Microtubule-based motors are supposed to be involved in transportation of muscle-specific proteins in differentiating myoblasts. The knowledge was generally based on the effect of microtubule inhibitors (Antin et al., 1981; Holtzer et al., 1975; Siebrands et al., 2004; Toyama et al., 1982). However, no direct evidence has been given to show the necessity of motors for specific cargo protein transportation. In our Kif5b-deficient myoblasts, the dispersion of α-sarcomeric actin, NMIIB, desmin and nestin to the growing tips was disturbed, and expression of Kif5b restored their localization. Actin and NMIIB exist in the premature myofilaments in growing tips of both differentiated skeletal myocytes and cardiac myocytes (LoRusso et al., 1997; Sanger et al., 2005); however, they aggregated in the central part

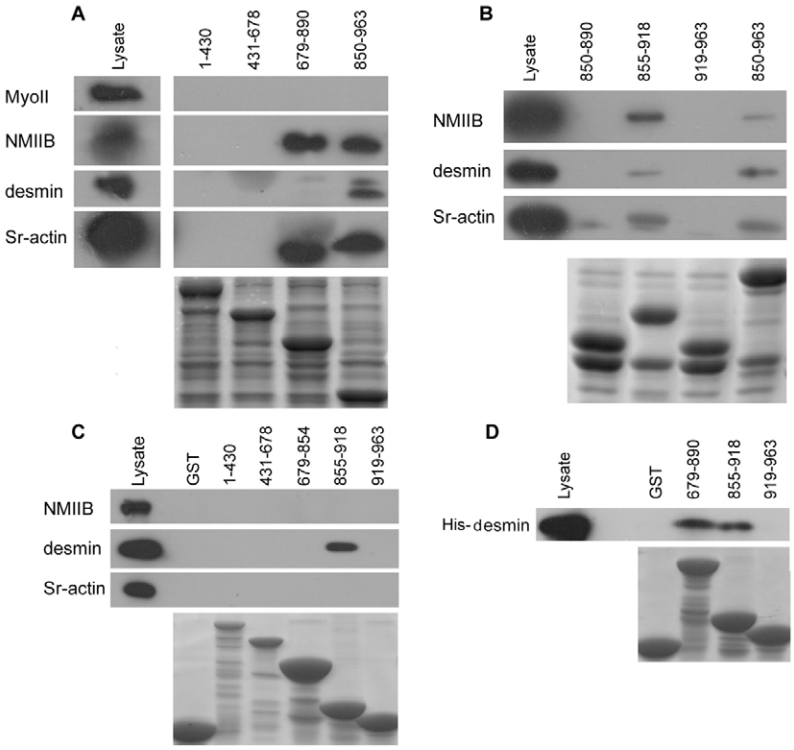

Fig. 8. Kif5b interacts with its cargo proteins through the 64-amino acid tail domain. (**A**,**B**) Kif5b fragments (A) or the fragments in the tail region (B) fused with GST were expressed from BL21 *E. coli* cells and then pulled-down using GST with lysate from wild-type myoblast cells differentiated for 2 days. (**C**) GST pull-down using lysate from mutant myoblast cells differentiated for 2 days. (**D**) His-tagged Desmin was expressed from BL21 *E. coli* cells and incubated with GST-Kif5b fusion proteins. Upper panel shows the western blot result and lower panel shows Coomassie Blue staining to show the expression of GST-Kif5b fusion proteins.

of Kif5b-deficient cells, which may directly affect the functional contractile unit formation. The growing tips, besides being a location for myofibril assembly, are important for cell-matrix interactions and resemble the sites of myotendinous junctions *in vivo*. The abolishment of the bipolar transportation of desmin and nestin by Kif5b deficiency may directly disrupt the linkage formation between the myofibrils and the MTJ. Besides, desmin has multiple functions, including in myofibrillogenesis, mitochondrial and nuclei localization (reviewed by Costa et al., 2004). Desmin mutation leads to filament deposition in cardiac and skeletal muscle cells, and causes skeletal muscle weakness and heart failure (Goldfarb et al., 2004); in particular, desmin mutations in the nebulin-binding domain destabilize actin filaments (Conover and Gregorio, 2011; Conover et al., 2009), indicating the importance of the proper localization and function of desmin. Therefore, the potential disruption of desmin and nestin functioning may also contribute to the myofibril, mitochondrial and nuclear phenotypes in Kif5b-deficient muscle cells.

At the molecular level, we demonstrated that Kif5b can associate with desmin directly through the proposed α-helix domain in the tail. The issue of whether Kif5b and nestin have a direct interaction requires further investigation. Type III and type IV IF proteins can form heteropolymers within one group or between the two groups, both *in vitro* and *in vivo* (reviewed by Herrmann and Aebi, 2000). Desmin, a type III IF protein, and nestin, a type IV IF protein, could form heteropolymers in muscles, suggesting that these proteins may form a complex on the microtubule highway to the cell tips. Actin and non-muscle myosin II can also form bundles based on the interaction between the head domain of non-muscle myosin II and actin (Conti and Adelstein, 2008), and desmin can bind to the giant actin-binding protein nebulin (Bang et al., 2002), raising the possibility that desmin may act as a direct linker of Kif5b to bind to the actin-associated myofibril components.

Taken together, our results reveal not only novel functions for kinesin-1 in myofibrillogenesis and MTJ formation, but also suggest roles for desmin and nestin dysfunction in the MTJ. We propose that kinesin-1 transports and/or tethers the IF proteins together with myofibril components in a complex to the myotube tips during myogenesis (summarized in Fig. 9). This model may

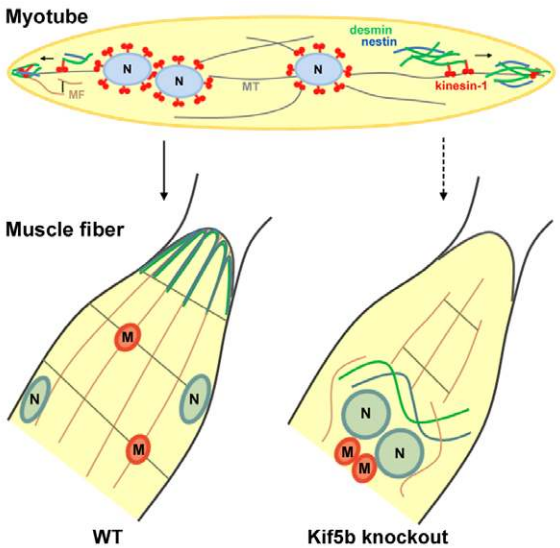

Fig. 9. Proposed model of Kif5b in myogenesis and the consequent defects in Kif5b-deficient skeletal muscles. Kif5b transports desmin/nestin together with some of the myofibril (MF) components along the microtubules (MTs) to the myotube tips during myogenesis by directly binding to desmin/nestin intermediate filaments. Kinesin-1 also functions in nuclei (N) and mitochondrial (M) positioning. In Kif5b-deficient skeletal muscle fibers, desmin/nestin cannot be transported to the myotendinous junction (MTJ) area and therefore mislocalizes around the nuclei in the cell body. Nuclei and mitochondria aggregate in the centre of the muscle cells. Myofibrils are rudimentally assembled or disassembled, and the formation of myofibril-MTJ linkage is severely disrupted.

provide new directions in studies of the molecular mechanisms of myofibrils assembly and MTJ-related diseases.

Acknowledgements
We thank Dr A. K. Groves for providing Pax2-Cre mice; Dr S. T. Brady for providing us the KLC antibodies KLC-All and 63-90, and mouse Kif5b cDNA; and Dr R. Adelstein for NMIIB antibody. We thank Dr Reinhard Fässler, Dr Neal G. Copeland and Dr Nancy A. Jenkins for their valuable comments on this work; Mr Jüergen Scharner for his help on the experiment and scientific discussions; Ms Alice Lui for her assistant of FACS analysis; Ms Jing Guo and Miss Jess Chan for technical support of confocal microscopy; and Mr W. S. Lee in Queen Mary Hospital for the EM microscopy.

Funding
This work was supported by grants from the Hong Kong Research Grants Council [HKU 7321/04M; HKU 7636/05M; HKU 767110M] and Hong Kong University Seed Funding Programme for Basic Research [200911159033] to J.D.H., and partially by an RGC Collaborative Research Fund [HKUST6/CRF/08].

Competing interests statement
The authors declare no competing financial interests.

Supplementary material
Supplementary material available online at
http://dev.biologists.org/lookup/suppl/doi:10.1242/dev.085969/-/DC1

References

Antin, P. B., Forry-Schaudies, S., Friedman, T. M., Tapscott, S. J. and Holtzer, H. (1981). Taxol induces postmitotic myoblasts to assemble interdigitating microtubule-myosin arrays that exclude actin filaments. *J. Cell Biol.* **90**, 300-308.
Argyropoulos, G., Stütz, A. M., Ilnytska, O., Rice, T., Teran-Garcia, M., Rao, D. C., Bouchard, C. and Rankinen, T. (2009). KIF5B gene sequence variation and response of cardiac stroke volume to regular exercise. *Physiol. Genomics* **36**, 79-88.
Bang, M. L., Gregorio, C. and Labeit, S. (2002). Molecular dissection of the interaction of desmin with the C-terminal region of nebulin. *J. Struct. Biol.* **137**, 119-127.
Carlsson, L., Li, Z., Paulin, D. and Thornell, L. E. (1999). Nestin is expressed during development and in myotendinous and neuromuscular junctions in wild type and desmin knock-out mice. *Exp. Cell Res.* **251**, 213-223.
Conover, G. M. and Gregorio, C. C. (2011). The desmin coil 1B mutation K190A impairs nebulin Z-disc assembly and destabilizes actin thin filaments. *J. Cell Sci.* **124**, 3464-3476.
Conover, G. M., Henderson, S. N. and Gregorio, C. C. (2009). A myopathy-linked desmin mutation perturbs striated muscle actin filament architecture. *Mol. Biol. Cell* **20**, 834-845.
Conti, M. A. and Adelstein, R. S. (2008). Nonmuscle myosin II moves in new directions. *J. Cell Sci.* **121**, 11-18.
Costa, M. L., Escaleira, R., Cataldo, A., Oliveira, F. and Mermelstein, C. S. (2004). Desmin: molecular interactions and putative functions of the muscle intermediate filament protein. *Braz. J. Med. Biol. Res.* **37**, 1819-1830.
Cui, J., Wang, Z., Cheng, Q., Lin, R., Zhang, X. M., Leung, P. S., Copeland, N. G., Jenkins, N. A., Yao, K. M. and Huang, J. D. (2011). Targeted inactivation of kinesin-1 in pancreatic β-cells in vivo leads to insulin secretory deficiency. *Diabetes* **60**, 320-330.
Diefenbach, R. J., Mackay, J. P., Armati, P. J. and Cunningham, A. L. (1998). The C-terminal region of the stalk domain of ubiquitous human kinesin heavy chain contains the binding site for kinesin light chain. *Biochemistry* **37**, 16663-16670.
Dietrich, K. A., Sindelar, C. V., Brewer, P. D., Downing, K. H., Cremo, C. R. and Rice, S. E. (2008). The kinesin-1 motor protein is regulated by a direct interaction of its head and tail. *Proc. Natl. Acad. Sci. USA* **105**, 8938-8943.
Dorner, C., Ciossek, T., Müller, S., Møller, P. H., Ullrich, A. and Lammers, R. (1998). Characterization of KIF1C, a new kinesin-like protein involved in vesicle transport from the Golgi apparatus to the endoplasmic reticulum. *J. Biol. Chem.* **273**, 20267-20275.
Faire, K., Gruber, D. and Bulinski, J. C. (1998). Identification of kinesin-like molecules in myogenic cells. *Eur. J. Cell Biol.* **77**, 27-34.
Gilbert, S. F. (2000). *Developmental Biology*, 6th edn. Sunderland, MA: Sinauer Associates.
Ginkel, L. M. and Wordeman, L. (2000). Expression and partial characterization of kinesin-related proteins in differentiating and adult skeletal muscle. *Mol. Biol. Cell* **11**, 4143-4158.
Glater, E. E., Megeath, L. J., Stowers, R. S. and Schwarz, T. L. (2006). Axonal transport of mitochondria requires milton to recruit kinesin heavy chain and is light chain independent. *J. Cell Biol.* **173**, 545-557.
Goldfarb, L. G., Vicart, P., Goebel, H. H. and Dalakas, M. C. (2004). Desmin myopathy. *Brain* **127**, 723-734.
Herrmann, H. and Aebi, U. (2000). Intermediate filaments and their associates: multi-talented structural elements specifying cytoarchitecture and cytodynamics. *Curr. Opin. Cell Biol.* **12**, 79-90.
Hirokawa, N., Pfister, K. K., Yorifuji, H., Wagner, M. C., Brady, S. T. and Bloom, G. S. (1989). Submolecular domains of bovine brain kinesin identified by electron microscopy and monoclonal antibody decoration. *Cell* **56**, 867-878.
Hollenbeck, P. J. (1989). The distribution, abundance and subcellular localization of kinesin. *J. Cell Biol.* **108**, 2335-2342.
Holtzer, H., Croop, J., Dienstman, S., Ishikawa, H. and Somlyo, A. P. (1975). Effects of cytochaslasin B and colcemide on myogenic cultures. *Proc. Natl. Acad. Sci. USA* **72**, 513-517.
Kaan, H. Y., Hackney, D. D. and Kozielski, F. (2011). The structure of the kinesin-1 motor-tail complex reveals the mechanism of autoinhibition. *Science* **333**, 883-885.
Kanai, Y., Dohmae, N. and Hirokawa, N. (2004). Kinesin transports RNA: isolation and characterization of an RNA-transporting granule. *Neuron* **43**, 513-525.
Kreitzer, G., Liao, G. and Gundersen, G. G. (1999). Detyrosination of tubulin regulates the interaction of intermediate filaments with microtubules in vivo via a kinesin-dependent mechanism. *Mol. Biol. Cell* **10**, 1105-1118.
LoRusso, S. M., Rhee, D., Sanger, J. M. and Sanger, J. W. (1997). Premyofibrils in spreading adult cardiomyocytes in tissue culture: evidence for reexpression of the embryonic program for myofibrillogenesis in adult cells. *Cell Motil. Cytoskeleton* **37**, 183-198.
Metzger, T., Gache, V., Xu, M., Cadot, B., Folker, E. S., Richardson, B. E., Gomes, E. R. and Baylies, M. K. (2012). MAP and kinesin-dependent nuclear positioning is required for skeletal muscle function. *Nature* **484**, 120-124.
Musa, H., Orton, C., Morrison, E. E. and Peckham, M. (2003). Microtubule assembly in cultured myoblasts and myotubes following nocodazole induced microtubule depolymerisation. *J. Muscle Res. Cell Motil.* **24**, 303-310.
Novak, A., Guo, C., Yang, W., Nagy, A. and Lobe, C. G. (2000). Z/EG, a double reporter mouse line that expresses enhanced green fluorescent protein upon Cre-mediated excision. *Genesis* **28**, 147-155.
Ohyama, T. and Groves, A. K. (2004). Generation of Pax2-Cre mice by modification of a Pax2 bacterial artificial chromosome. *Genesis* **38**, 195-199.
Prahlad, V., Yoon, M., Moir, R. D., Vale, R. D. and Goldman, R. D. (1998). Rapid movements of vimentin on microtubule tracks: kinesin-dependent assembly of intermediate filament networks. *J. Cell Biol.* **143**, 159-170.
Rahkila, P., Väänänen, K., Saraste, J. and Metsikkö, K. (1997). Endoplasmic reticulum to Golgi trafficking in multinucleated skeletal muscle fibers. *Exp. Cell Res.* **234**, 452-464.
Rando, T. A. and Blau, H. M. (1994). Primary mouse myoblast purification, characterization, and transplantation for cell-mediated gene therapy. *J. Cell Biol.* **125**, 1275-1287.
Roux, K. J., Crisp, M. L., Liu, Q., Kim, D., Kozlov, S., Stewart, C. L. and Burke, B. (2009). Nesprin 4 is an outer nuclear membrane protein that can induce kinesin-mediated cell polarization. *Proc. Natl. Acad. Sci. USA* **106**, 2194-2199.
Sanger, J. W., Kang, S., Siebrands, C. C., Freeman, N., Du, A., Wang, J., Stout, A. L. and Sanger, J. M. (2005). How to build a myofibril. *J. Muscle Res. Cell Motil.* **26**, 343-354.
Siebrands, C. C., Sanger, J. M. and Sanger, J. W. (2004). Myofibrillogenesis in skeletal muscle cells in the presence of taxol. *Cell Motil. Cytoskeleton* **58**, 39-52.
Tanaka, Y., Kanai, Y., Okada, Y., Nonaka, S., Takeda, S., Harada, A. and Hirokawa, N. (1998). Targeted disruption of mouse conventional kinesin heavy chain, kif5B, results in abnormal perinuclear clustering of mitochondria. *Cell* **93**, 1147-1158.
Tassin, A. M., Maro, B. and Bornens, M. (1985). Fate of microtubule-organizing centers during myogenesis in vitro. *J. Cell Biol.* **100**, 35-46.
Tidball, J. G. (1992). Desmin at myotendinous junctions. *Exp. Cell Res.* **199**, 206-212.
Towler, M. C., Gleeson, P. A., Hoshino, S., Rahkila, P., Manalo, V., Ohkoshi, N., Ordahl, C., Parton, R. G. and Brodsky, F. M. (2004). Clathrin isoform CHC22, a component of neuromuscular and myotendinous junctions, binds sorting nexin 5 and has increased expression during myogenesis and muscle regeneration. *Mol. Biol. Cell* **15**, 3181-3195.
Toyama, Y., Forry-Schaudies, S., Hoffman, B. and Holtzer, H. (1982). Effects of taxol and Colcemid on myofibrillogenesis. *Proc. Natl. Acad. Sci. USA* **79**, 6556-6560.
Wang, X. and Schwarz, T. L. (2009). The mechanism of Ca2+-dependent regulation of kinesin-mediated mitochondrial motility. *Cell* **136**, 163-174.
Xia, C. H., Roberts, E. A., Her, L. S., Liu, X., Williams, D. S., Cleveland, D. W. and Goldstein, L. S. (2003). Abnormal neurofilament transport caused by targeted disruption of neuronal kinesin heavy chain KIF5A. *J. Cell Biol.* **161**, 55-66.
Yabe, J. T., Pimenta, A. and Shea, T. B. (1999). Kinesin-mediated transport of neurofilament protein oligomers in growing axons. *J. Cell Sci.* **112**, 3799-3814.
Yang, J. T., Laymon, R. A. and Goldstein, L. S. (1989). A three-domain structure of kinesin heavy chain revealed by DNA sequence and microtubule binding analyses. *Cell* **56**, 879-889.